Structural Engineering and Mechanics, *Vol. 60, No. 4 (2016) 707-727*
DOI: http://dx.doi.org/10.12989/sem.2016.60.4.707

A four-variable plate theory for thermal vibration of embedded FG nanoplates under non-uniform temperature distributions with different boundary conditions

Mohammad Reza Barati and Hossein Shahverdi*

Aerospace Engineering Department & Center of Excellence in Computational Aerospace, AmirKabir University of Technology, Tehran 15875-4413, Iran

(Received December 19, 2015, Revised August 9, 2016, Accepted September 30, 2016)

Abstract. In this paper, thermal vibration of a nonlocal functionally graded (FG) plates with arbitrary boundary conditions under linear and non-linear temperature fields is explored by developing a refined shear deformation plate theory with an inverse cotangential function in which shear deformation effect was involved without the need for shear correction factors. The material properties of FG nanoplate are considered to be temperature-dependent and graded in the thickness direction according to the Mori-Tanaka model. On the basis of non-classical higher order plate model and Eringen's nonlocal elasticity theory, the small size influence was captured. Numerical examples show the importance of non-uniform thermal loadings, boundary conditions, gradient index, nonlocal parameter and aspect and side-to-thickness ratio on vibrational responses of size-dependent FG nanoplates.

Keywords: thermal vibration; four-variable plate theory; functionally graded nanoplate; nonlocal elasticity theory; elastic foundation

1. Introduction

Structures composed of functionally graded materials (FGMs) have been increasingly applied in the field of aerospace, mechanic and civil engineering due to possessing beneficial features. However, these structures are often exposed to severe thermo-mechanical loads during their operational life, so that the temperature rise indicates notable impact on the mechanical behavior of FGM structures (Barati, Zenkour *et al*. 2016). As a consequence, carefully evaluation of thermal effects on the behavior of FGM structures under various thermo-mechanical loadings is a key issue. To this purpose, several papers are published incorporating the high-order displacement terms with transverse displacements, for analysis of FGM plates to overcome the defects of classical plate theory (CPT) which neglects the influences of shear deformation and overestimates natural frequencies (Bouiadjra, Bedia *et al*. 2013). For example, Javaheri and Eslami (2002) derived the equilibrium and stability equations of FGM based rectangular plates under thermal loads, based on the higher order shear deformation plate theory. Recently refined two-variable plate theory develop by Shimpi (2002) has been gained a great attention from many authors (Kim,

*Corresponding author, Ph.D., E-mail: h_shahverdi@aut.ac.ir

http://www.techno-press.org/?journal=sem&subpage=8 ISSN: 1225-4568 (Print), 1598-6217 (Online)

plate theory develop by Shimpi (2002) has been gained a great attention from many authors (Kim, Thai *et al*. 2009, Narendar 2011, Thai and Kim 2012, Sobhy 2014, 2015a, 2015b, Mechab, Atmane *et al*. 2010). The refined two-variable plate theory is extended by several researchers to contain four unknown functions (Thai and Choi 2011, Bourada, Tounsi *et al*. 2012, Tounsi, Houari *et al*. 2013, Sobhy 2016). The refined four-variable plate theory accounts for a higher order variation of the transverse shear strains in the thickness direction and mentioned that the number of independent unknowns of the theory is four, as against five in other shear deformation theories. Also, Zenkour and Sobhy (2011) analyzed thermal stability of FGM plates embedded in two-parameter Pasternak's foundations based upon the trigonometric shear deformation plate theory. Also, Ta and Noh (2015) presented analytical solution of the dynamic behavior of FG rectangular plates embedded in elastic medium using a new refined plate theory. Most recently, Kulkarni *et al*. (2015) developed a shear deformation theory named as inverse cotangential shear deformation theory (ICSDT) for functionally graded macro plates. They showed that inverse cotangential shear deformation theory provide accurate results in analysis of FG plates. Therefore, examination of accuracy of this theory has not examined in vibration analysis of FG nanoplates till to now.

Recently, nano-size structures have extensively been applied for development of Nanoelectromechanical systems (NEMS) such as nanosensors and nanoactuators. On the other hand, due to shortcomings of classical continuum theories in accurate description of the size-dependent behavior of nano-scale structures, the investigators have attempted to propose appropriate theories for this purpose. In this manner, the nonlocal theory of elasticity by Eringen (Eringen and Edelen 1972, Eringen 1983) is the most cited theory which has the potential to consider the scale effects on the mechanical responses of nanostructures. To extend nonlocal elasticity theory for analysis of FG structures, vibrational behavior of nanosize (FG) beams via finite element method was explored by Eltaher, Emam *et al*. (2012). Also, based on finite element method scale-dependent linear free vibrational behavior of functionally graded (FG) nanoplates is investigated by Natarajan, Chakraborty *et al*. (2012). In this work, the nonlocal constitutive relation based on Eringen's differential form of nonlocal elasticity theory was applied. The resonance behaviors of FG micro/nano plates using Kirchhoff plate theory was studied by Nami and Janghorban (2014). In this study, they adopted the nonlocal elasticity theory and strain gradient theory with one gradient parameter to consider the small scale effects. Daneshmehr and Rajabpoor (2014) presented a nonlocal higher order plate theory for stability analysis of FG nanoplates subjected to biaxial in plane loadings using Generalized Differential Quadrature (GDQ) method. Based on a modified couple stress theory, a model for sigmoid functionally graded material (S-FGM) nanoplates on elastic medium is developed by Jung, Han *et al*. (2014). Most recently, Ebrahimi and Barati (2015) proposed a nonlocal third order beam model for vibration analysis of FG nanobeams. Also, based on surface elasticity theory, Ansari, Ashrafi *et al*. (2015) investigated the buckling and vibration responses of nanoplates made of FGMs subjected to a linear thermal loading in pre-buckling domain with considering the effect of surface stress. Zare, Nazemnezhad *et al*. (2015) determined the natural frequencies of a FG nanoplate for different combinations of boundary conditions. Recently, Sobhy (2015c) presented a comprehensive study on FGM nanoplates embedded in an elastic medium using an analytical method.

It is apparent that the temperature-dependency effect is disregarded in all of the above-mentioned studies on FG nanoplates. Therefore, a work to investigate various thermal loadings effects on vibrational behavior of nano-scale FG plates with temperature-dependent material properties in both pre-buckling and post-buckling regions has not been published up to now. In fact, a significant change in material properties is reported when the FGM based structures are

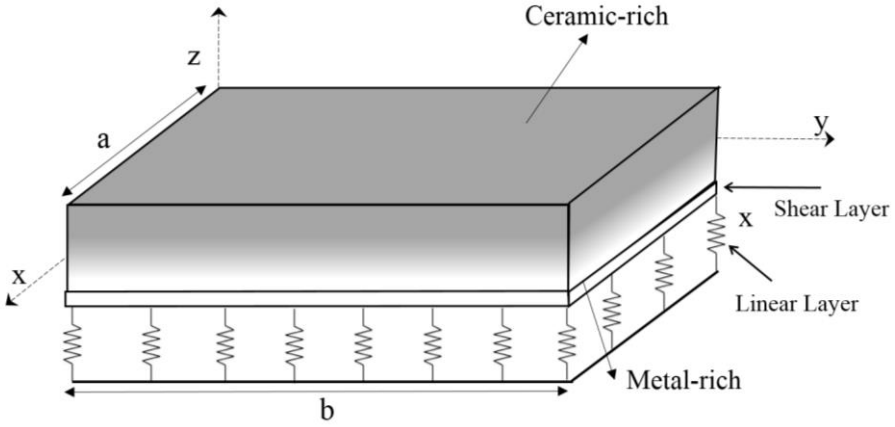

Fig. 1 Geometry and coordinates of functionally graded nanoplate

under high temperature environments. For example, Young's modulus usually reduces due to temperature rise. To more accurate anticipation of FGMs behavior exposed to vigorous temperatures, consideration of temperature dependency on the material properties is very necessary. Furthermore, due to the expansion of new technologies, especially nanotechnology, a number of systems and structures may experience severe thermal environments, resulting in various kinds of thermal loads. Therefore, creating a text is necessitated which focuses on the thermal vibration analysis of such nanostructures. As a destructive phenomenon, thermo-mechanical vibration must be analyzed to ensure the safety of size-dependent structures.

This study investigates the effects of non-uniform thermal loadings on vibration characteristics of size-dependent functionally graded (FG) nanoplates resting on elastic foundation near the post-buckling region. FG nanoplate is modeled via a refined four-variable shear deformation theory with an inverse cotangential function so that doesn't require any shear correction factor. The material properties of FG nanoplate are assumed to be dependent on both temperature and spatial coordinate based on Mori-Tanaka homogenization scheme. The related formulations are derived using extended Hamilton's principle in conjunction with Eringen's nonlocal elasticity theory. The proposed analytical solution which satisfies simply-supported, clamped and free boundary conditions and some combinations of them is used to solve the equations. The reliability of the present plate model and solution procedure is verified with those published works. The effects of elastic foundation, temperature-dependency, various thermal loads, small scale parameter and gradient index on vibration of thermally pre/post buckled FG nanoplates are figured out and presented.

2. Theory and formulation

2.1 Mori-Tanaka (MT) FGM plate model

Material properties of FGMs are supposed to change according to a Mori-Tanaka model about spatial coordinates. The coordinate system for FG nanoplate is shown in Fig. 1. The FG nanoplate is assumed to be combination of ceramic and metal and effective material properties (P_f) of the FG

plate such as Young's modulus E_f is supposed to change continuously in the direction of z-axis (thickness direction) according to an power function of the volume fractions of the material constituents. So, the effective material properties, P_f can be stated as

$$P_f = P_c V_c + P_m V_m \tag{1}$$

where subscripts m and c denote metal and ceramic, respectively and the volume fraction of the ceramic is associated to that of the metal in the following relation:

$$V_c + V_m = 1 \tag{2.a}$$

The volume fraction of the ceramic constituent of the plate is assumed to be given by:

$$V_c = \left(\frac{z}{h} + \frac{1}{2}\right)^p \tag{2.b}$$

in which p is gradient index and determines the material composition through the thickness. According to Mori-Tanaka homogenization technique the local effective material properties of the FG nanoplate such as effective local bulk modulus K_e and shear modulus μ_e can be calculated

$$\frac{K_e - K_m}{K_c - K_m} = \frac{V_c}{1 + V_m (K_c - K_m)/(K_m + 4\mu_m/3)} \tag{3.a}$$

$$\frac{\mu_e - \mu_m}{\mu_c - \mu_m} = \frac{V_c}{1 + V_m (\mu_c - \mu_m)/[(\mu_m + \mu_m (9K_m + 8\mu_m)/(6(K_m + 2\mu_m))]} \tag{3.b}$$

Therefore from Eq. (3), the effective Young's modulus (E), Poisson's ratio (v) based on Mori-Tanaka scheme can be expressed by

$$E(z,T) = \frac{9K_e \mu_e}{3K_e + \mu_e} \tag{4}$$

$$v(z,T) = \frac{3K_e - 2\mu_e}{6K_e + 2\mu_e} \tag{5}$$

Also, The thermal expansion coefficient (α) and thermal conductivity (κ) may be expressed by

$$\frac{\alpha_e - \alpha_m}{\alpha_c - \alpha_m} = \frac{\frac{1}{K_e} - \frac{1}{K_m}}{\frac{1}{K_c} - \frac{1}{K_m}} \tag{6}$$

$$\frac{\kappa_e - \kappa_m}{\kappa_c - \kappa_m} = \frac{V_c}{1 + V_m \frac{(\kappa_c - \kappa_m)}{3\kappa_m}} \tag{7}$$

The material composition of the FG nanoplate at the upper surface (z=+h/2) is supposed to be the pure ceramic and it changes continuously to the opposite side surface (z=-h/2) which is pure metal as it is shown in Fig. 1.

For more precise prediction of FGMs behavior under severe temperature, material properties

Table 1 Temperature-dependent coefficients for Si_3N_4 and SUS304 (Shen and Wang 2015)

Material	Properties	P_0	P_{-1}	P_1	P_2	P_3
Si_3N_4	E (Pa)	348.43e+9	0	-3.070e-4	2.160e-7	-8.946e-11
	α (K^{-1})	5.8723e-6	0	9.095e-4	0	0
	ρ (Kg/m^3)	2370	0	0	0	0
	κ (W/mK)	13.723	0	-1.032e-3	5.466e-7	-7.876e-11
	ν	0.24	0	0	0	0
SUS304	E (Pa)	201.04e+9	0	3.079e-4	-6.534e-7	0
	α (K^{-1})	12.330e-6	0	8.086e-4	0	0
	ρ (Kg/m^3)	8166	0	0	0	0
	κ (W/mK)	15.379	0	-1.264e-3	2.092e-6	-7.223e-10
	ν	0.3262	0	-2.002e-4	3.797e-7	0

should be dependent on temperature. The non-linear equation of thermo-elastic material properties in function of temperature T (K) can be stated as (Touloukian 1967)

$$P = P_0(P_{-1}T^{-1} + 1 + P_1T + P_2T^2 + P_3T^3) \tag{8}$$

where P_0, P_{-1}, P_1, P_2 and P_3 denote the temperature dependent coefficients of material properties, according to those given in Table 1, of Si_3N_4 and SUS304.

2.2 Kinematic relations

Non-polynomial shear deformation theory recently developed by Kulkarni, Singh *et al*. (2015) for FG plates which has five field variables has extended for FG nanoplates and the number of unknowns are reduced based on the four-variable plate theory. Hence, the displacement field at any point of the plate can be written as

$$u_1(x,y,z,t) = u(x,y,t) - z\frac{\partial w_b}{\partial x} - f(z)\frac{\partial w_s}{\partial x} \tag{9}$$

$$u_2(x,y,z,t) = v(x,y,t) - z\frac{\partial w_b}{\partial y} - f(z)\frac{\partial w_s}{\partial y} \tag{10}$$

$$u_3(x,y,z,t) = w_b(x,y,t) + w_s(x,y,t) \tag{11}$$

where the theory has an inverse cotangential function in the form

$$f(z) = z - \Psi(z) + \Omega z \tag{12-a}$$

and

$$\Psi(z) = \cot^{-1}(rh/z) \tag{12-b}$$

$$\Omega = 4r/[h(4r^2+1)] \tag{12-c}$$

with r=0.46. Also, u and v are displacement components of the mid-surface and w_b and w_s are the bending and shear transverse displacement, respectively. Nonzero strains of the four-variable plate model are expressed as follows

$$\begin{Bmatrix}\varepsilon_x\\ \varepsilon_y\\ \gamma_{xy}\end{Bmatrix}=\begin{Bmatrix}\varepsilon_x^0\\ \varepsilon_y^0\\ \gamma_{xy}^0\end{Bmatrix}+z\begin{Bmatrix}\kappa_x^b\\ \kappa_y^b\\ \kappa_{xy}^b\end{Bmatrix}+f(z)\begin{Bmatrix}\kappa_x^s\\ \kappa_y^s\\ \kappa_{xy}^s\end{Bmatrix},\ \begin{Bmatrix}\gamma_{yz}\\ \gamma_{xz}\end{Bmatrix}=g(z)\begin{Bmatrix}\gamma_{yz}^s\\ \gamma_{xz}^s\end{Bmatrix} \tag{13}$$

where $g(z)=1-df/dz$ and

$$\begin{Bmatrix}\varepsilon_x^0\\ \varepsilon_y^0\\ \gamma_{xy}^0\end{Bmatrix}=\begin{Bmatrix}\frac{\partial u}{\partial x}\\ \frac{\partial v}{\partial y}\\ \frac{\partial u}{\partial y}+\frac{\partial v}{\partial x}\end{Bmatrix},\ \begin{Bmatrix}\kappa_x^b\\ \kappa_y^b\\ \kappa_{xy}^b\end{Bmatrix}=\begin{Bmatrix}-\frac{\partial^2 w_b}{\partial x^2}\\ -\frac{\partial^2 w_b}{\partial y^2}\\ -2\frac{\partial^2 w_b}{\partial x\partial y}\end{Bmatrix},\ \begin{Bmatrix}\kappa_x^s\\ \kappa_y^s\\ \kappa_{xy}^s\end{Bmatrix}=\begin{Bmatrix}-\frac{\partial^2 w_s}{\partial x^2}\\ -\frac{\partial^2 w_s}{\partial y^2}\\ -2\frac{\partial^2 w_s}{\partial x\partial y}\end{Bmatrix},\ \begin{Bmatrix}\gamma_{yz}^s\\ \gamma_{xz}^s\end{Bmatrix}=\begin{Bmatrix}\frac{\partial w_s}{\partial y}\\ \frac{\partial w_s}{\partial x}\end{Bmatrix} \tag{14}$$

Through extended Hamilton's principle, in which the motion of an elastic structure in the time interval $t1<t<t2$ is so that the integral with respect to time of the total potential energy is extremum

$$\int_0^t \delta(U-T+V)dt=0 \tag{15}$$

here, U is strain energy, T is kinetic energy and V is work done by external forces. The first variation of the strain energy can be calculated as

$$\delta U=\int_v \sigma_{ij}\delta\varepsilon_{ij}\,dV=\int_v(\sigma_x\delta\varepsilon_x+\sigma_y\delta\varepsilon_y+\sigma_{xy}\delta\gamma_{xy}+\sigma_{yz}\delta\gamma_{yz}+\sigma_{xz}\delta\gamma_{xz})\,dV \tag{16}$$

Substituting Eqs. (13) and (14) into Eq. (16) yields

$$\begin{aligned}\delta U=\int_0^a\int_0^b[&N_x\frac{\partial\delta u}{\partial x}-M_x^b\frac{\partial^2\delta w_b}{\partial x^2}-M_x^s\frac{\partial^2\delta w_s}{\partial x^2}+N_y\frac{\partial\delta v}{\partial y}-M_y^b\frac{\partial^2\delta w_b}{\partial y^2}-M_y^s\frac{\partial^2\delta w_s}{\partial y^2}\\ &+N_{xy}(\frac{\partial\delta u}{\partial y}+\frac{\partial\delta v}{\partial x})-2M_{xy}^b\frac{\partial^2\delta w_b}{\partial x\partial y}-2M_{xy}^s\frac{\partial^2\delta w_s}{\partial x\partial y}+Q_{yz}\frac{\partial\delta w_s}{\partial y}+Q_{xz}\frac{\partial\delta w_s}{\partial x}]dxdy\end{aligned} \tag{17}$$

In which the variables introduced in arriving at the last expression are defined as follows

$$\begin{aligned}&(N_i,M_i^b,M_i^s)=\int_{-h/2}^{h/2}(1,z,f)\sigma_i dz,\ i=(x,y,xy)\\ &Q_i=\int_{-h/2}^{h/2}g(z)\sigma_i dz,\ i=(xz,yz)\end{aligned} \tag{18}$$

The first variation of the work done by applied forces can be written in the following form

$$\begin{aligned}\delta V=\int_0^a\int_0^b(&N_x^0\frac{\partial(w_b+w_s)}{\partial x}\frac{\partial\delta(w_b+w_s)}{\partial x}+N_y^0\frac{\partial(w_b+w_s)}{\partial y}\frac{\partial\delta(w_b+w_s)}{\partial y}\\ &+2\delta N_{xy}^0\frac{\partial(w_b+w_s)}{\partial x}\frac{\partial(w_b+w_s)}{\partial y}-k_w\delta(w_b+w_s)\\ &+k_p(\frac{\partial\delta(w_b+w_s)}{\partial x}\frac{\partial(w_b+w_s)}{\partial x}+\frac{\partial\delta(w_b+w_s)}{\partial y}\frac{\partial(w_b+w_s)}{\partial y}))dxdy\end{aligned} \tag{19}$$

where N_x^0, N_y^0, N_{xy}^0 are in-plane applied loads and k_w, k_p are elastic foundation parameters. The first variation of the kinetic energy can be written in the form

$$\delta K = \int_0^a \int_0^b [I_0(\frac{\partial u}{\partial t}\frac{\partial \delta u}{\partial t} + \frac{\partial v}{\partial t}\frac{\partial \delta v}{\partial t} + \frac{\partial (w_b + w_s)}{\partial t}\frac{\partial \delta (w_b + w_s)}{\partial t}) - I_1(\frac{\partial u}{\partial t}\frac{\partial \delta w_b}{\partial x \partial t} + \frac{\partial w_b}{\partial x \partial t}\frac{\partial \delta u}{\partial t} + \frac{\partial v}{\partial t}\frac{\partial \delta w_b}{\partial y \partial t}$$
$$+ \frac{\partial w_b}{\partial y \partial t}\frac{\partial \delta v}{\partial t}) - J_1(\frac{\partial u}{\partial t}\frac{\partial \delta w_s}{\partial x \partial t} + \frac{\partial w_s}{\partial x \partial t}\frac{\partial \delta u}{\partial t} + \frac{\partial v}{\partial t}\frac{\partial \delta w_s}{\partial y \partial t} + \frac{\partial w_s}{\partial y \partial t}\frac{\partial \delta v}{\partial t}) + I_2(\frac{\partial w_b}{\partial x \partial t}\frac{\partial \delta w_b}{\partial x \partial t} + \frac{\partial w_b}{\partial y \partial t}\frac{\partial \delta w_b}{\partial y \partial t})$$
$$+ K_2(\frac{\partial w_s}{\partial x \partial t}\frac{\partial \delta w_s}{\partial x \partial t} + \frac{\partial w_s}{\partial y \partial t}\frac{\partial \delta w_s}{\partial y \partial t}) + J_2(\frac{\partial w_b}{\partial x \partial t}\frac{\partial \delta w_s}{\partial x \partial t} + \frac{\partial w_s}{\partial x \partial t}\frac{\partial \delta w_b}{\partial x \partial t} + \frac{\partial w_b}{\partial y \partial t}\frac{\partial \delta w_s}{\partial y \partial t} + \frac{\partial w_s}{\partial y \partial t}\frac{\partial \delta w_b}{\partial y \partial t})]dxdy \tag{20}$$

in which I_0, I_1, J_1, I_2, J_2 and K_2 are mass inertia statements which defined as

$$(I_0, I_1, J_1, I_2, J_2, K_2) = \int_{-h/2}^{h/2} \rho(z)(1, z, f, z^2, zf, f^2)dz \tag{21}$$

By inserting Eqs. (17)-(20) into Eq. (15) and setting the coefficients of δu, δv, δw_b and δw_s to zero, the following Euler–Lagrange equations can be obtained

$$\frac{\partial N_x}{\partial x} + \frac{\partial N_{xy}}{\partial y} = I_0 \frac{\partial^2 u}{\partial t^2} - I_1 \frac{\partial^3 w_b}{\partial x \partial t^2} - J_1 \frac{\partial^3 w_s}{\partial x \partial t^2} \tag{22}$$

$$\frac{\partial N_{xy}}{\partial x} + \frac{\partial N_y}{\partial y} = I_0 \frac{\partial^2 v}{\partial t^2} - I_1 \frac{\partial^3 w_b}{\partial y \partial t^2} - J_1 \frac{\partial^3 w_s}{\partial y \partial t^2} \tag{23}$$

$$\begin{aligned} &\frac{\partial^2 M_x^b}{\partial x^2} + 2\frac{\partial^2 M_{xy}^b}{\partial x \partial y} + \frac{\partial^2 M_y^b}{\partial y^2} - k_w(w_b + w_s) + k_p \nabla^2 (w_b + w_s) - N^T \nabla^2 (w_b + w_s) \\ &= I_0 \frac{\partial^2 (w_b + w_s)}{\partial t^2} + I_1(\frac{\partial^3 u}{\partial x \partial t^2} + \frac{\partial^3 v}{\partial y \partial t^2}) - I_2 \nabla^2 (\frac{\partial^2 w_b}{\partial t^2}) - J_2 \nabla^2 (\frac{\partial^2 w_s}{\partial t^2}) \end{aligned} \tag{24}$$

$$\begin{aligned} &\frac{\partial^2 M_x^s}{\partial x^2} + 2\frac{\partial^2 M_{xy}^s}{\partial x \partial y} + \frac{\partial^2 M_y^s}{\partial y^2} + \frac{\partial Q_{xz}}{\partial x} + \frac{\partial Q_{yz}}{\partial y} - k_w(w_b + w_s) + k_p \nabla^2 (w_b + w_s) - N^T \nabla^2 (w_b + w_s) \\ &= I_0 \frac{\partial^2 (w_b + w_s)}{\partial t^2} + J_1(\frac{\partial^3 u}{\partial x \partial t^2} + \frac{\partial^3 v}{\partial y \partial t^2}) - J_2 \nabla^2 (\frac{\partial^2 w_b}{\partial t^2}) - K_2 \nabla^2 (\frac{\partial^2 w_s}{\partial t^2}) \end{aligned} \tag{25}$$

where $N_x^0 = N_y^0 = N^T, N_{xy}^0 = 0$ and thermal resultant can be expressed as

$$N^T = \int_{-h/2}^{h/2} \frac{E(z,T)}{1 - \nu(z,T)} \alpha(z,T)(T - T_0)\, dz \tag{26}$$

2.3 The nonlocal elasticity model for FG nanobeam

According to Eringen nonlocal elasticity model (Eringen and Edelen 1972) which contains wide range interactions between points in a continuum solid, the stress state at a point inside a body is regarded to be function of all neighbor points' strains. Hence, in the present work in order

to capture the small size impacts nonlocal elasticity theory is implemented in which a linear differential framework of constitutive equations is expressed as

$$(1-(e_0a)\nabla^2)\sigma_{kl}=t_{kl} \tag{27}$$

In which ∇^2 denotes the Laplacian operator. Therefore, the scale length e_0a considers the influences of small size on the response of nano-scale structures. Thus, the constitutive relations of nonlocal theory for a higher order FG nanoplate can be stated as

$$(1-\mu\nabla^2)\begin{Bmatrix}\sigma_x\\ \sigma_y\\ \sigma_{xy}\\ \sigma_{yz}\\ \sigma_{xz}\end{Bmatrix}=\begin{pmatrix}Q_{11} & Q_{12} & 0 & 0 & 0\\ Q_{12} & Q_{22} & 0 & 0 & 0\\ 0 & 0 & Q_{66} & 0 & 0\\ 0 & 0 & 0 & Q_{44} & 0\\ 0 & 0 & 0 & 0 & Q_{55}\end{pmatrix}\begin{Bmatrix}\varepsilon_x-\alpha\Delta T\\ \varepsilon_y-\alpha\Delta T\\ \gamma_{xy}\\ \gamma_{yz}\\ \gamma_{xz}\end{Bmatrix} \tag{28}$$

also

$$Q_{11}=Q_{22}=\frac{E(z,T)}{1-\nu^2(z,T)},\ Q_{12}=\nu(z)Q_{11},\ Q_{44}=Q_{55}=Q_{66}=\frac{E(z,T)}{2(1+\nu(z,T))} \tag{29}$$

where $\mu=(e_0a)^2$. Integrating Eq. (28) over the plate's cross-section area, one can obtain the force-strain and the moment-strain of the nonlocal refined FG plates as follows

$$(1-\mu\nabla^2)\begin{Bmatrix}N_x\\ N_y\\ N_{xy}\end{Bmatrix}=\begin{pmatrix}A_{11} & A_{12} & 0\\ A_{12} & A_{22} & 0\\ 0 & 0 & A_{66}\end{pmatrix}\begin{Bmatrix}\frac{\partial u}{\partial x}\\ \frac{\partial v}{\partial y}\\ \frac{\partial u}{\partial y}+\frac{\partial v}{\partial x}\end{Bmatrix}+\begin{pmatrix}B_{11} & B_{12} & 0\\ B_{12} & B_{22} & 0\\ 0 & 0 & B_{66}\end{pmatrix}\begin{Bmatrix}-\frac{\partial^2 w_b}{\partial x^2}\\ -\frac{\partial^2 w_b}{\partial y^2}\\ -2\frac{\partial^2 w_b}{\partial x\partial y}\end{Bmatrix}+\begin{pmatrix}B_{11}^s & B_{12}^s & 0\\ B_{12}^s & B_{22}^s & 0\\ 0 & 0 & B_{66}^s\end{pmatrix}\begin{Bmatrix}-\frac{\partial^2 w_s}{\partial x^2}\\ -\frac{\partial^2 w_s}{\partial y^2}\\ -2\frac{\partial^2 w_s}{\partial x\partial y}\end{Bmatrix} \tag{30}$$

$$(1-\mu\nabla^2)\begin{Bmatrix}M_x^b\\ M_y^b\\ M_{xy}^b\end{Bmatrix}=\begin{pmatrix}B_{11} & B_{12} & 0\\ B_{12} & B_{22} & 0\\ 0 & 0 & B_{66}\end{pmatrix}\begin{Bmatrix}\frac{\partial u}{\partial x}\\ \frac{\partial v}{\partial y}\\ \frac{\partial u}{\partial y}+\frac{\partial v}{\partial x}\end{Bmatrix}+\begin{pmatrix}D_{11} & D_{12} & 0\\ D_{12} & D_{22} & 0\\ 0 & 0 & D_{66}\end{pmatrix}\begin{Bmatrix}-\frac{\partial^2 w_b}{\partial x^2}\\ -\frac{\partial^2 w_b}{\partial y^2}\\ -2\frac{\partial^2 w_b}{\partial x\partial y}\end{Bmatrix}+\begin{pmatrix}D_{11}^s & D_{12}^s & 0\\ D_{12}^s & D_{22}^s & 0\\ 0 & 0 & D_{66}^s\end{pmatrix}\begin{Bmatrix}-\frac{\partial^2 w_s}{\partial x^2}\\ -\frac{\partial^2 w_s}{\partial y^2}\\ -2\frac{\partial^2 w_s}{\partial x\partial y}\end{Bmatrix} \tag{31}$$

$$(1-\mu\nabla^2)\begin{Bmatrix}M_x^s\\ M_y^s\\ M_{xy}^s\end{Bmatrix}=\begin{pmatrix}B_{11}^s & B_{12}^s & 0\\ B_{12}^s & B_{22}^s & 0\\ 0 & 0 & B_{66}^s\end{pmatrix}\begin{Bmatrix}\frac{\partial u}{\partial x}\\ \frac{\partial v}{\partial y}\\ \frac{\partial u}{\partial y}+\frac{\partial v}{\partial x}\end{Bmatrix}+\begin{pmatrix}D_{11}^s & D_{12}^s & 0\\ D_{12}^s & D_{22}^s & 0\\ 0 & 0 & D_{66}^s\end{pmatrix}\begin{Bmatrix}-\frac{\partial^2 w_b}{\partial x^2}\\ -\frac{\partial^2 w_b}{\partial y^2}\\ -2\frac{\partial^2 w_b}{\partial x\partial y}\end{Bmatrix}+\begin{pmatrix}H_{11}^s & H_{12}^s & 0\\ H_{12}^s & H_{22}^s & 0\\ 0 & 0 & H_{66}^s\end{pmatrix}\begin{Bmatrix}-\frac{\partial^2 w_s}{\partial x^2}\\ -\frac{\partial^2 w_s}{\partial y^2}\\ -2\frac{\partial^2 w_s}{\partial x\partial y}\end{Bmatrix} \tag{32}$$

$$(1-\mu\nabla^2)\begin{Bmatrix} Q_x \\ Q_y \end{Bmatrix} = \begin{pmatrix} A_{44}^s & 0 \\ 0 & A_{55}^s \end{pmatrix} \begin{Bmatrix} \frac{\partial w_s}{\partial x} \\ \frac{\partial w_s}{\partial y} \end{Bmatrix} \tag{33}$$

In which the cross-sectional rigidities are defined as follows

$$\begin{Bmatrix} A_{11}, B_{11}, B_{11}^s, D_{11}, D_{11}^s, H_{11}^s \\ A_{12}, B_{12}, B_{12}^s, D_{12}, D_{12}^s, H_{12}^s \\ A_{66}, B_{66}, B_{66}^s, D_{66}, D_{66}^s, H_{66}^s \end{Bmatrix} = \int_{-h/2}^{h/2} Q_{11}(1, z, f, z^2, zf, f^2) \begin{Bmatrix} 1 \\ \nu(z,T) \\ \frac{1-\nu(z,T)}{2} \end{Bmatrix} dz \tag{34}$$

$$A_{44}^s = A_{55}^s = \int_{-h/2}^{h/2} (g^2(z) \frac{E(z,T)}{2(1+\nu(z,T))}) dz \tag{35}$$

The nonlocal governing equations of refined four-variable shear deformation FG nanoplate in terms of the displacement can be derived by substituting Eqs. (30)-(33), into Eqs. (22)-(25) as follows

$$\begin{aligned} &A_{11}\frac{\partial^2 u}{\partial x^2} + A_{66}\frac{\partial^2 u}{\partial y^2} + (A_{12}+A_{66})\frac{\partial^2 v}{\partial x \partial y} - B_{11}\frac{\partial^3 w_b}{\partial x^3} - (B_{12}+2B_{66})\frac{\partial^3 w_b}{\partial x \partial y^2} - B_{11}^s\frac{\partial^3 w_s}{\partial x^3} \\ &-(B_{12}^s+2B_{66}^s)\frac{\partial^3 w_s}{\partial x \partial y^2} + (1-\mu\nabla^2)(-I_0\frac{\partial^2 u}{\partial t^2} + I_1\frac{\partial^3 w_b}{\partial x \partial t^2} + J_1\frac{\partial^3 w_s}{\partial x \partial t^2}) = 0 \end{aligned} \tag{36}$$

$$\begin{aligned} &A_{66}\frac{\partial^2 v}{\partial x^2} + A_{22}\frac{\partial^2 v}{\partial y^2} + (A_{12}+A_{66})\frac{\partial^2 u}{\partial x \partial y} - B_{22}\frac{\partial^3 w_b}{\partial y^3} - (B_{12}+2B_{66})\frac{\partial^3 w_b}{\partial x^2 \partial y} - B_{22}^s\frac{\partial^3 w_s}{\partial y^3} \\ &-(B_{12}^s+2B_{66}^s)\frac{\partial^3 w_s}{\partial x^2 \partial y} + (1-\mu\nabla^2)(-I_0\frac{\partial^2 v}{\partial t^2} + I_1\frac{\partial^3 w_b}{\partial y \partial t^2} + J_1\frac{\partial^3 w_s}{\partial y \partial t^2}) = 0 \end{aligned} \tag{37}$$

$$\begin{aligned} &B_{11}\frac{\partial^3 u}{\partial x^3} + (B_{12}+2B_{66})\frac{\partial^3 u}{\partial x \partial y^2} + (B_{12}+2B_{66})\frac{\partial^3 v}{\partial x^2 \partial y} + B_{22}\frac{\partial^3 v}{\partial y^3} - D_{11}\frac{\partial^4 w_b}{\partial x^4} - D_{22}\frac{\partial^4 w_b}{\partial y^4} \\ &-2(D_{12}+2D_{66})\frac{\partial^4 w_b}{\partial x^4 \partial y^2} - D_{11}^s\frac{\partial^4 w_s}{\partial x^4} - 2(D_{12}^s+2D_{66}^s)\frac{\partial^4 w_s}{\partial x^4 \partial y^2} - D_{22}^s\frac{\partial^4 w_s}{\partial y^4} \\ &+(1-\mu\nabla^2)(I_0\frac{\partial^2 (w_b+w_s)}{\partial t^2} + I_1(\frac{\partial^3 u}{\partial x \partial t^2} + \frac{\partial^3 v}{\partial y \partial t^2}) - I_2\nabla^2(\frac{\partial^2 w_b}{\partial t^2}) - J_2\nabla^2(\frac{\partial^2 w_s}{\partial t^2}) \\ &-N^T\nabla^2(w_b+w_s) - k_w(w_b+w_s) + k_p\nabla^2(w_b+w_s)) = 0 \end{aligned} \tag{38}$$

$$\begin{aligned} &B_{11}^s\frac{\partial^3 u}{\partial x^3} + (B_{12}^s+2B_{66}^s)\frac{\partial^3 u}{\partial x \partial y^2} + (B_{12}^s+2B_{66}^s)\frac{\partial^3 v}{\partial x^2 \partial y} + B_{22}^s\frac{\partial^3 v}{\partial y^3} - D_{11}^s\frac{\partial^4 w_b}{\partial x^4} + A_{55}^s\frac{\partial^2 w_s}{\partial x^2} \\ &+A_{44}^s\frac{\partial^2 w_s}{\partial y^2} - 2(D_{12}^s+2D_{66}^s)\frac{\partial^4 w_b}{\partial x^4 \partial y^2} - D_{22}^s\frac{\partial^4 w_b}{\partial y^4} - H_{11}^s\frac{\partial^4 w_s}{\partial x^4} - 2(H_{12}^s+2H_{66}^s)\frac{\partial^4 w_s}{\partial x^4 \partial y^2} \\ &-H_{22}^s\frac{\partial^4 w_s}{\partial y^4} + (1-\mu\nabla^2)(I_0\frac{\partial^2 (w_b+w_s)}{\partial t^2} + J_1(\frac{\partial^3 u}{\partial x \partial t^2} + \frac{\partial^3 v}{\partial y \partial t^2}) - J_2\nabla^2(\frac{\partial^2 w_b}{\partial t^2}) - K_2\nabla^2(\frac{\partial^2 w_s}{\partial t^2}) \\ &-N^T\nabla^2(w_b+w_s) - k_w(w_b+w_s) + k_p\nabla^2(w_b+w_s)) = 0 \end{aligned} \tag{39}$$

It should be mentioned that by setting μ=0, a local thermo-mechanical vibration analysis of FG plates is rendered.

3. Solution procedures

In this section, an analytical solution of the nonlocal governing equations for free vibration of a FG nanoplate with the following relations of simply-supported (*S*), clamped (*C*) or free (*F*) edges or some combinations of them is presented (Sobhy 2013):

Simply-supported (S):

$w_b = w_s = N_x = M_x = 0$ at x=0, *a*

$w_b = w_s = N_y = M_y = 0$ at y=0, *b*

Clamped (C):

$u = v = w_b = w_s = 0$ at x=0, *a* and y=0, *b*

Free (F):

$M_x = M_{xy} = Q_{xz} = 0$ at x=0, *a*

$M_y = M_{xy} = Q_{yz} = 0$ at y=0, *b*

To satisfy aforementioned boundary conditions, the displacement quantities are presented in the following form

$$u = \sum_{m=1}^{\infty}\sum_{n=1}^{\infty} U_{mn} \frac{\partial X_m(x)}{\partial x} Y_n(y) e^{i\omega_n t} \tag{40}$$

$$v = \sum_{m=1}^{\infty}\sum_{n=1}^{\infty} V_{mn} X_m(x) \frac{\partial Y_n(y)}{\partial y} e^{i\omega_n t} \tag{41}$$

$$w_b = \sum_{m=1}^{\infty}\sum_{n=1}^{\infty} W_{bmn} X_m(x) Y_n(y) e^{i\omega_n t} \tag{42}$$

$$w_s = \sum_{m=1}^{\infty}\sum_{n=1}^{\infty} W_{smn} X_m(x) Y_n(y) e^{i\omega_n t} \tag{43}$$

where (U_{mn}, V_{mn}, W_{bmn}, W_{smn}) are the unknown coefficients and the approximate functions X_m and Y_n are tabulated in detail in Table 3 for different boundary conditions ($\lambda=m\pi/a$, $\beta=n\pi/b$). Inserting Eqs. (40)-(43) into Eqs. (36)-(39) respectively, leads to

$$\left\{ \begin{pmatrix} k_{1,1} & k_{1,2} & k_{1,3} & k_{1,4} \\ k_{2,1} & k_{2,2} & k_{2,3} & k_{2,4} \\ k_{3,1} & k_{3,2} & k_{3,3} & k_{3,4} \\ k_{4,1} & k_{4,2} & k_{4,3} & k_{4,4} \end{pmatrix} - \bar{\omega}_n^{\,2} \begin{pmatrix} m_{1,1} & m_{1,2} & m_{1,3} & m_{1,4} \\ m_{2,1} & m_{2,2} & m_{2,3} & m_{2,4} \\ m_{3,1} & m_{3,2} & m_{3,3} & m_{3,4} \\ m_{4,1} & m_{4,2} & m_{4,3} & m_{4,4} \end{pmatrix} \right\} \begin{Bmatrix} U_{mn} \\ V_{mn} \\ W_{bmn} \\ W_{smn} \end{Bmatrix} = 0 \tag{44}$$

where

$$
\begin{aligned}
&k_{1,1}=A_{11}\kappa_{12}+A_{66}\kappa_8,\ \ k_{1,2}=\left(A_{12}+A_{66}\right)\kappa_8,\ \ k_{1,3}=-B_{11}\kappa_{12}-\left(B_{12}+2B_{66}\right)\kappa_8,\ \ k_{1,4}=-B^s_{11}\kappa_{12}-\left(B^s_{12}+2B^s_{66}\right)\kappa_8,\\
&k_{2,2}=A_{22}\kappa_4+A_{66}\kappa_{10},\ \ k_{2,3}=-B_{22}\kappa_4-\left(B_{12}+2B_{66}\right)\kappa_{10},\ \ k_{2,4}=-B^s_{22}\kappa_4-\left(B^s_{12}+2B^s_{66}\right)\kappa_{10},\\
&k_{3,3}=-D_{11}\kappa_{13}-2\left(D_{12}+2D_{66}\right)\kappa_{11}-D_{22}\kappa_5-K_w\kappa_1+(-N^T+K_p-\mu K_w)\left(\kappa_3+\kappa_9\right)+\mu(N^T-K_p)\left(\kappa_5+\kappa_{13}+2\kappa_{11}\right),\\
&k_{3,4}=-D^s_{11}\kappa_{13}-2\left(D^s_{12}+2D^s_{66}\right)\kappa_{11}-D^s_{22}\kappa_5-K_w\kappa_1+(-N^T+K_p-\mu K_w)\left(\kappa_3+\kappa_9\right)+\mu(N^T-K_p)\left(\kappa_5+\kappa_{13}+2\kappa_{11}\right),\\
&k_{4,4}=-H^s_{11}\kappa_{13}-2\left(H^s_{12}+2H^s_{66}\right)\kappa_{11}-H^s_{22}\kappa_5+A^s_{44}\kappa_9+A^s_{55}\kappa_3-K_w\kappa_1+(-N^T+K_p-\mu K_w)\left(\kappa_3+\kappa_9\right)+\mu(N^T-K_p)\left(\kappa_5+\kappa_{13}+2\kappa_{11}\right),\\
&m_{1,1}=+I_0\kappa_6-\mu I_0\left(\kappa_{12}+\kappa_8\right),\ \ m_{1,3}=+I_1\kappa_9-I_1\mu\left(\kappa_{13}+\kappa_{11}\right),\ \ m_{1,4}=+J_1\kappa_9-J_1\mu\left(\kappa_{13}+\kappa_{11}\right),\\
&m_{2,2}=+I_0\kappa_2-\mu I_0\left(\kappa_{10}+\kappa_4\right),\ \ m_{2,3}=+I_1\kappa_3-I_1\mu\left(\kappa_{11}+\kappa_5\right),\ \ m_{2,4}=+J_1\kappa_3-J_1\mu\left(\kappa_{11}+\kappa_5\right),\\
&\{m_{3,3},m_{3,4},m_{4,4}\}=+I_0\kappa_1-\{I_2,J_2,K_2\}\left(\kappa_3+\kappa_9\right)-\mu I_0\left(\kappa_3+\kappa_9\right)+\mu\{I_2,J_2,K_2\}\left(\kappa_5+\kappa_{13}+2\kappa_{11}\right),
\end{aligned}
\tag{45}
$$

in which

$$
\begin{aligned}
(\kappa_1,\kappa_3,\kappa_5)&=\int_0^a\int_0^b(X_mY_n,X_mY_n'',X_mY_n'''')X_mY_n\,dxdy\\
(\kappa_9,\kappa_{11},\kappa_{13})&=\int_0^a\int_0^b(X_m''Y_n,X_m''Y_n'',X_m''''Y_n)X_mY_n\,dxdy\\
(\kappa_6,\kappa_8,\kappa_{12})&=\int_0^a\int_0^b(X_m'Y_n,X_m'Y_n'',X_m'''Y_n)X_m'Y_n\,dxdy\\
(\kappa_2,\kappa_4,\kappa_{10})&=\int_0^a\int_0^b(X_mY_n',X_mY_n''',X_m''Y_n')X_mY_n'\,dxdy
\end{aligned}
\tag{46}
$$

4. Types of thermal loading

4.1 Linear Temperature Rise (LTR)

When the plate thickness is thin enough, the temperature distribution is supposed to be varied linearly through the thickness as follows (Javaheri and Eslami 2002)

$$T=T_m+\Delta T\left(\frac{1}{2}+\frac{z}{h}\right) \tag{47}$$

where the temperature difference in Eq. (47) is $\Delta T=T_c-T_m$ and T_c and T_m are the temperature of the top surface and the bottom surface, respectively.

4.2 Nonlinear temperature rise (NLTR)

The temperature distribution through-the-thickness can be obtained by solving the steady-state heat conduction equation with the boundary conditions on bottom and top surfaces of the plate

$$
\begin{aligned}
&-\frac{d}{dz}\left(\kappa(z,T)\frac{dT}{dz}\right)=0\\
&T\left(\frac{h}{2}\right)=T_c,\ \ T\left(-\frac{h}{2}\right)=T_m
\end{aligned}
\tag{48}
$$

Table 2 Displacement models applied in analysis of nanoplates

Model	Theory	Number of unknown functions
CPT	Classical plate theory	3
FSDT	First-order shear deformation theory (Natarajan, Chakraborty *et al*. 2012)	5
TSDT	Third-order shear deformation theory (Daneshmehr and Rajabpoor 2014)	5
SSDT	Sinusoidal shear deformation theory	5
present	Refined inverse cotangential shear deformation theory	4

Table 3 The admissible functions $X_m(x)$ and $Y_n(y)$ (Sobhy 2013)

	Boundary conditions		The functions X_m and Y_n	
	At x=0, a	At y=0, b	$X_m(x)$	$Y_n(y)$
SSSS	$X_m(0)=X_m''(0)=0$ $X_m(a)=X_m''(a)=0$	$Y_n(0)=Y_n''(0)=0$ $Y_n(b)=Y_n''(b)=0$	$Sin(\lambda x)$	$Sin(\beta y)$
CSSS	$X_m(0)=X_m'(0)=0$ $X_m(a)=X_m''(a)=0$	$Y_n(0)=Y_n''(0)=0$ $Y_n(b)=Y_n''(b)=0$	$Sin(\lambda x)[Cos(\lambda x)-1]$	$Sin(\beta y)$
CSCS	$X_m(0)=X_m'(0)=0$ $X_m(a)=X_m''(a)=0$	$Y_n(0)=Y_n'(0)=0$ $Y_n(b)=Y_n''(b)=0$	$Sin(\lambda x)[Cos(\lambda x)-1]$	$Sin(\beta y)[Cos(\beta y)-1]$
CCSS	$X_m(0)=X_m'(0)=0$ $X_m(a)=X_m'(a)=0$	$Y_n(0)=Y_n''(0)=0$ $Y_n(b)=Y_n''(b)=0$	$Sin^2(\lambda x)$	$Sin(\beta y)$
CCCC	$X_m(0)=X_m'(0)=0$ $X_m(a)=X_m'(a)=0$	$Y_n(0)=Y_n'(0)=0$ $Y_n(b)=Y_n'(b)=0$	$Sin^2(\lambda x)$	$Sin^2(\beta y)$
FFCC	$X_m''(0)=X_m'''(0)=0$ $X_m''(a)=X_m'''(a)=0$	$Y_n(0)=Y_n'(0)=0$ $Y_n(b)=Y_n'(b)=0$	$Cos^2(\lambda x)[Sin^2(\lambda x)+1]$	$Sin^2(\beta y)$

The solution of above equation is

$$T = T_m + \Delta T \frac{\int_{-\frac{h}{2}}^{z} \frac{1}{\kappa(z,T)} dz}{\int_{-\frac{h}{2}}^{\frac{h}{2}} \frac{1}{\kappa(z,T)} dz} \tag{49}$$

where $\Delta T=T_c-T_m$.

5. Numerical results and discussions

Here, the thermo-mechanical vibration behavior of temperature-dependent FG nanoplates embedded in two-parameter elastic foundation is studied using a new four-variable shear deformation theory with an inverse cotangential function. The temperature-dependent material properties of the nonlocal FG plate vary through the thickness direction according to Mori-Tanaka

Table 4 Comparison of non-dimensional fundamental natural frequency of Mori-Tanaka based FG nanoplates with simply-supported and clamped boundary conditions (p=5)

a/h	μ	SSSS				CCCC			
		a/b=1		a/b=2		a/b=1		a/b=2	
		Natarajan, Chakraborty *et al.* (2012)	present	Natarajan, Chakraborty *et al.* (2012)	present	Natarajan, Chakraborty *et al.* (2012)	present	Natarajan, Chakraborty *et al.* (2012)	present
10	0	0.0441	0.043823	0.1055	0.104329	0.0758	0.078893	0.1789	0.189380
	1	0.0403	0.040070	0.0863	0.085493	0.0682	0.070135	0.1426	0.146338
	2	0.0374	0.037141	0.0748	0.074174	0.0624	0.063767	0.1218	0.123547
	4	0.0330	0.032806	0.0612	0.060673	0.0542	0.054949	0.0978	0.098461
20	0	0.0113	0.011256	0.0279	0.027756	0.0207	0.020954	0.0534	0.054706
	1	0.0103	0.010288	0.0229	0.022722	0.0186	0.018639	0.0422	0.042393
	2	0.0096	0.009534	0.0198	0.019704	0.0170	0.016953	0.0358	0.035836
	4	0.0085	0.008418	0.0162	0.016110	0.0147	0.014615	0.0287	0.028592

homogenization technique. Different plate theories available in the literature and their displacement models are tabulated in Table 2 to show the novelty of the present plate theory. Numerical results are provided to indicate the influences of non-uniform thermal loads (LTR and NLTR), nonlocal parameter, Winkler and Pasternak constants, gradient index and aspect ratio on the vibration responses of a FG nanoplate. Also a 5 (K) increase in metal surface to reference temperature T_0 of the nanoscale FG plate is considered, i.e., $T_m - T_0 = 5(K)$ (Javaheri and Eslami 2002). To evaluate the correctness of the present results, dimensionless frequency of FG nanoplates with simply-supported and clamped boundary conditions are compared with those obtained by Natarajan, Chakraborty *et al*. (2012) through first order shear deformation theory and finite element method and the results are provided in Table 4. For comparison study, the material properties are selected as: $\rho_c = 2370\ kg/m^3$, E_c = 348.43 GPa, $\rho_m = 8166\ kg/m^3$, E_m = 201.04 GPa and v=0.3. Also, for better presentation of the obtained results the following dimensionless quantities are adopted

$$\hat{\omega} = \omega \frac{a^2}{h}\sqrt{\frac{\rho_c}{E_c}},\ K_w = \frac{k_w a^4}{D_c}, K_p = \frac{k_p a^2}{D_c}, D_c = \frac{E_c h^3}{12(1-v_c^2)} \tag{50}$$

To provide extensive numerical results, Tables 5 and 6 present the influences of Winkler and Pasternak elastic foundation constants (K_w, K_p), non-uniform thermal loadings, nonlocal parameter and gradient index on the thermal vibration frequency of temperature-dependent nonlocal square FG plates with various boundary conditions (SSSS, CSSS, CSCS, CCSS, CCCC and FFCC) at a/h=20. A rise in Winkler or Pasternak parameter of elastic foundation leads to larger values of dimensionless frequency for all cases of thermal loads and boundary conditions. The reason is higher rigidity of the nanoplate when it is in contact with elastic foundation. Contrary to elastic foundation, the presence of nonlocality results in reduction in plate stiffness and natural frequencies. For a prescribed thermal condition and gradient index, the SSSS FG nanoplate has the smallest dimensionless frequency and FFCC has the largest one. Also, it is found that non-linear temperature rise (NLTR) provides higher natural frequency than LTR.

Table 5 The variation of the non-dimensional fundamental frequency of the FG nanoplate subjected to linear temperature rise (LTR) with various boundary conditions

B.C.	μ	ΔT=20 [K]			ΔT=50 [K]			ΔT=100 [K]		
		(K_w, K_p)			(K_w, K_p)			(K_w, K_p)		
		(0,0)	(25,0)	(25,5)	(0,0)	(25,0)	(25,5)	(0,0)	(25,0)	(25,5)
SSSS	0	3.44673	3.58768	4.09643	3.35201	3.4966	4.01691	3.17557	3.32783	3.87090
	1	3.13288	3.28723	3.83604	3.02823	3.20457	3.72257	2.83228	3.03498	3.59353
	2	2.88694	3.05368	3.63789	2.77263	2.97748	3.49619	2.55684	2.80614	3.38069
CSSS	0	4.96129	5.06041	5.53929	4.87787	4.97822	5.46431	4.72300	4.82657	5.32651
	1	4.40175	4.52309	5.0265	4.30244	4.43527	4.94762	4.15578	4.27315	4.80282
	2	3.98932	4.12965	4.65657	3.87565	4.03641	4.57409	3.73376	3.86399	4.42268
CSCS	0	6.27653	6.35536	6.82865	6.19686	6.27606	6.75491	6.04826	6.12939	6.61886
	1	5.44137	5.54508	6.0549	5.34130	5.45784	5.97511	5.15632	5.29683	5.82841
	2	4.85954	4.9835	5.52715	4.74172	4.88887	5.44198	4.52323	4.71417	5.28560
CCSS	0	5.20360	5.29784	5.71185	5.13257	5.22809	5.64722	5.00126	5.09924	5.52815
	1	4.67335	4.77804	5.24655	4.59080	4.69733	5.17315	4.40867	4.54842	5.03832
	2	4.27266	4.38691	4.90268	4.17970	4.29642	4.82188	3.95174	4.12927	4.67357
CCCC	0	6.53188	6.60787	6.99072	6.46919	6.54534	6.93164	6.35162	6.42900	6.82190
	1	5.77745	5.86286	6.37626	5.68932	5.77541	6.29596	5.52644	5.61399	6.14822
	2	5.22555	5.31955	5.94018	5.11548	5.21079	5.84300	4.91178	5.00985	5.66453
FFCC	0	6.95121	7.02282	7.36586	6.89624	6.96784	7.31347	6.79244	6.86489	7.21545
	1	6.18065	6.26862	6.72617	6.09684	6.19208	6.6549	5.94184	6.60505	6.52334
	2	5.60955	5.71139	6.26403	5.50094	5.61634	6.1775	5.30012	5.44091	6.01844

Table 6 The variation of the non-dimensional fundamental frequency of the FG nanoplate subjected to heat conduction (NLTR) with various boundary conditions

B.C.	μ	ΔT=20 [K]			ΔT=50 [K]			ΔT=100 [K]		
		(K_w, K_p)			(K_w, K_p)			(K_w, K_p)		
		(0,0)	(25,0)	(25,5)	(0,0)	(25,0)	(25,5)	(0,0)	(25,0)	(25,5)
SSSS	0	3.44911	3.5898	4.09829	3.35852	3.50285	4.02235	3.19279	3.34427	3.88504
	1	3.14424	3.29801	3.80331	3.05267	3.21082	3.72796	2.88465	3.05152	3.59167
	2	2.90591	3.07166	3.57674	2.81285	2.98378	3.50156	2.64155	2.82287	3.3655
CSSS	0	4.96371	5.06236	5.54107	4.88369	4.98392	5.4695	4.73805	4.8413	5.33986
	1	4.41449	4.52516	5.02835	4.32852	4.44133	4.95305	4.17197	4.2889	4.81684
	2	4.0103	4.13183	4.6585	3.91853	4.04282	4.57975	3.75111	3.88076	4.43734
CSCS	0	6.2791	6.35727	6.83043	6.20249	6.28162	6.76007	6.06272	6.14365	6.63207
	1	5.45735	5.54715	6.0568	5.3727	5.46389	5.98064	5.21863	5.31247	5.84263
	2	4.88561	4.98573	5.52916	4.79339	4.8954	5.44785	4.62551	4.73114	5.30074
CCSS	0	5.2053	5.29951	5.7134	5.13754	5.23297	5.65173	5.01403	5.11176	5.5397
	1	4.6753	4.77995	5.24829	4.59652	4.70292	5.17822	4.45314	4.56288	5.05138
	2	4.27484	4.38903	4.90458	4.1861	4.30265	4.82743	4.02442	4.14552	4.68793
CCCC	0	6.53415	6.6094	6.99216	6.47384	6.54979	6.93584	6.3631	6.44035	6.8326
	1	5.78921	5.87396	6.34416	5.71232	5.7982	6.27408	5.5722	5.6602	6.14678
	2	5.24469	5.33806	5.88153	5.15336	5.24835	5.80024	4.98712	5.08522	5.65306
FFCC	0	6.9534	7.02418	7.36717	6.90048	6.9718	7.31724	6.80263	6.87497	7.22504
	1	6.19116	6.27046	6.72789	6.11719	6.19745	6.65989	5.9822	6.06424	6.53611
	2	5.62656	5.71364	6.26609	5.53441	5.62293	6.18348	5.36671	5.45794	6.03385

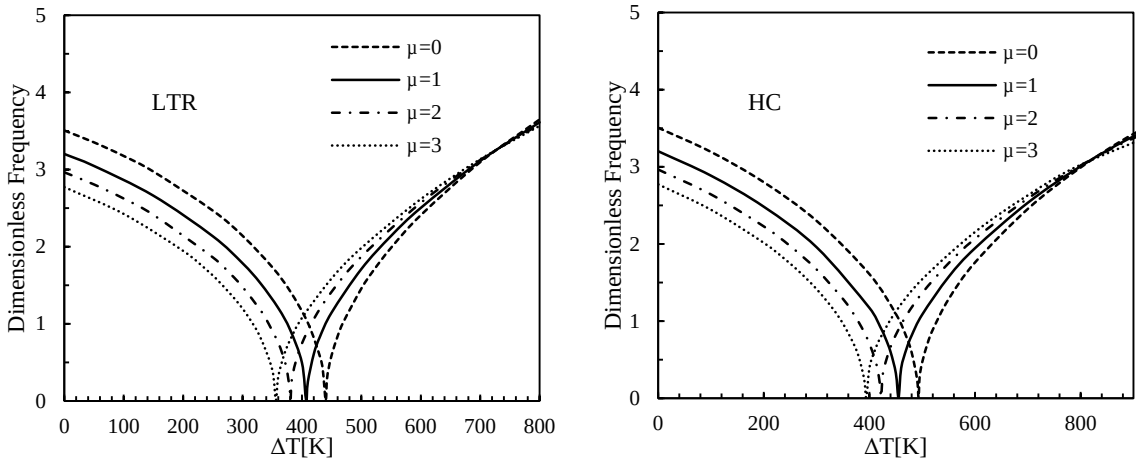

Fig. 2 Influence of nonlocal parameter on the dimensionless frequency of the foundationless SSSS square FG nanoplate with respect to various temperature rises (p=1, a/h=20, K_w=K_p=0)

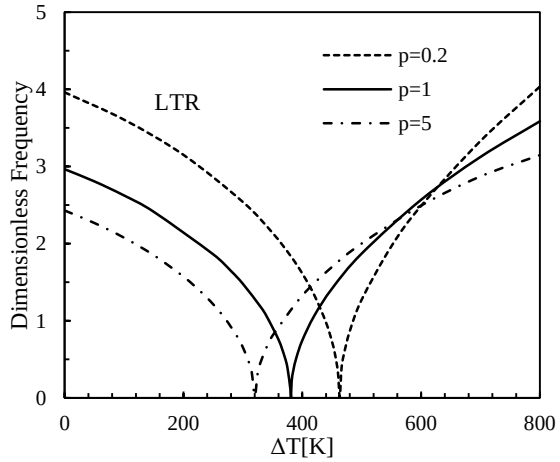

Fig. 3 Influence of gradient index on the dimensionless frequency of FG nanoplate for different thermal loadings (μ=2, a/h=20, K_w=K_p=0)

Figs. 2 and 3 respectively present the influences of small scale parameter and gradient index on the variation of dimensionless frequency of temperature-dependent square FG nanoplates versus various temperature rises at a/h=20. When μ=0 and p=0 the plate behavior is similar to those of homogenous macro scale plates. It should be mentioned that with the temperature increment, the natural frequency of FG nanoplates reaches to zero nearby the critical temperature point. This feature refers to stiffness degradation of a nanoplate when the temperature growths. After the critical temperature, the nanoplate continues to vibrating and increasing in temperature yields in larger values of natural frequency. Both nonlocality and gradient index have a softening impact on the rigidity of the nanoplate and reduce the dimensionless frequency. Hence, the branching point is shifted to the left with the increase of nonlocal parameter and gradient index.

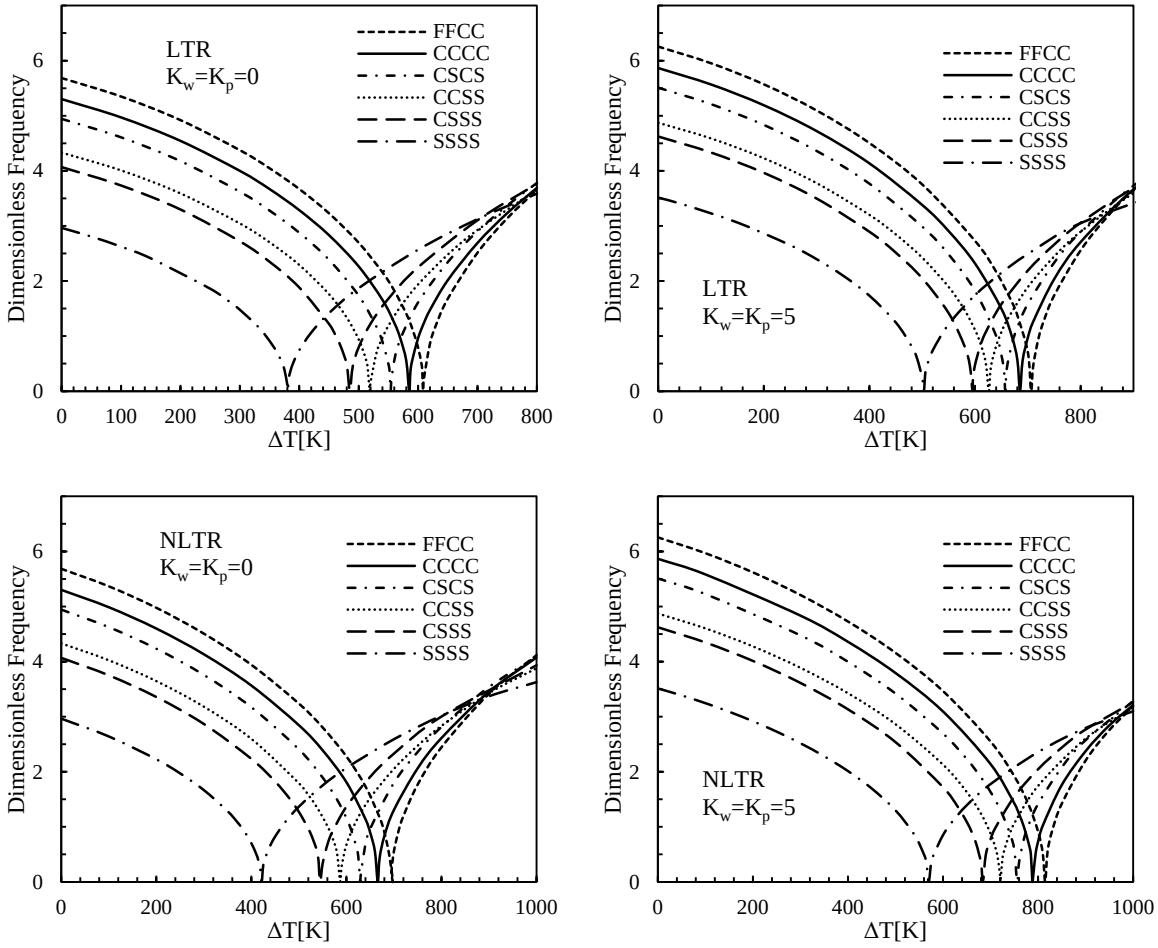

Fig. 4 Variation of the dimensionless frequency of FG nanoplate with and without elastic foundation versus various temperature rises for different boundary conditions (μ=2, p=1, a/h=20)

The variation of dimensionless frequency of square FG nanoplates with and without elastic foundation versus various temperature changes for different boundary conditions at μ=2 nm^2, p=1 and a/h=20 is illustrated in Fig. 4. As it is shown in this figure, the elastic foundation possesses remarkable capability to postpone the critical point of the nanostructure for all cases of thermal loads. Also, FFCC and SSSS FG nanoplates provide the highest and lowest values of critical temperature point. Therefore, boundary condition has a key factor for utilization of FG nanoplates in thermal environments.

To present the effects of elastic foundation parameters individually. Figs. 5 and 6 show the variation of dimensionless frequency with respect to Winkler and Pasternak constants, respectively, at a/h=20 and p=1 for both local (μ=0) and nonlocal (μ=2) plates with various temperature rises. It is observable that Winkler and Pasternak constants exhibit an increasing effect on the natural frequency by possessing a hardening influence on the plate structure. More, precisely it is clear that the shear layer or Pasternak-type foundation has a more considerable

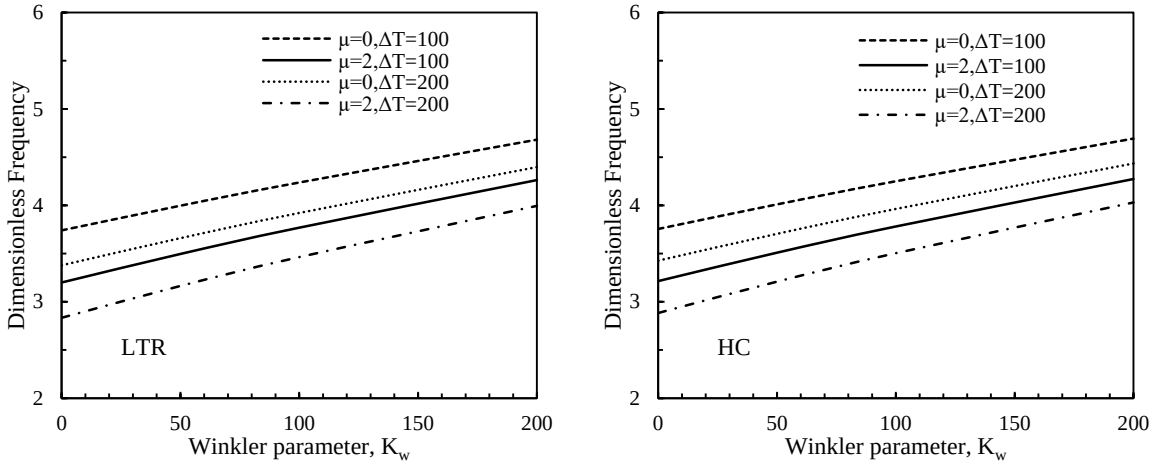

Fig. 5 Influence of the linear layer of elastic foundation on the dimensionless frequency of FG nanoplate for different thermal loadings (p=1, a/h=20)

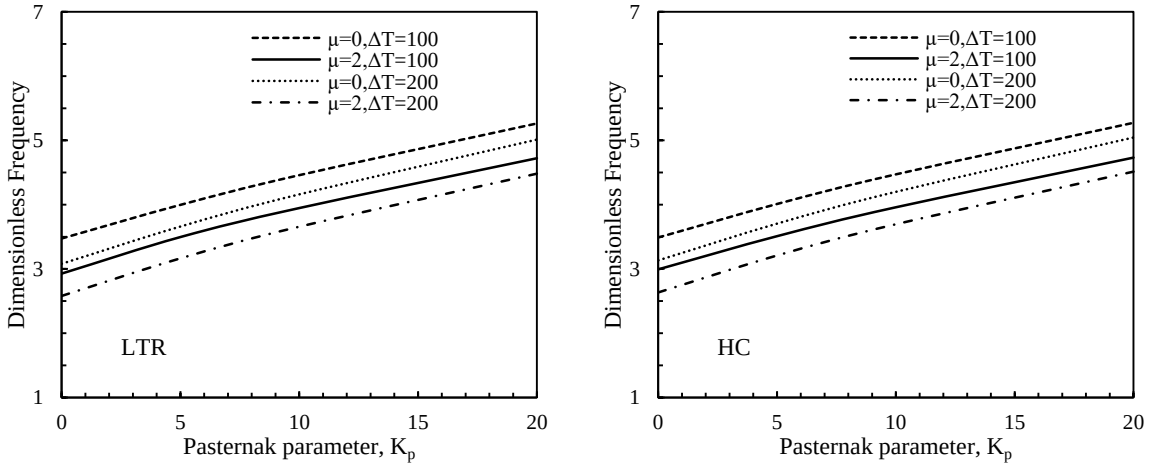

Fig. 6 Influence of the shear layer of elastic foundation on the dimensionless frequency of FG nanoplate for different thermal loadings (p=1, a/h=20)

impact on the dimensionless frequency than Winkler-type foundation.

The non-dimensional frequency of FG nanoplates with arbitrary boundary conditions as a function of gradient index at ΔT=100(K) of various temperature rises when μ=2 nm^2 is plotted in Fig. 7. According to the former discussions, gradient index has a reducing effect on the natural frequency of FG nanoplates. Here, it is shown that for all kinds of boundary edges at a specified contact conditions, the lower values of gradient index have more significant influence on the reduction of frequency, while the higher values of gradient index have no sensible effect on the frequency.

Figs. 8 and 9 demonstrate the influence of plate side-to-thickness ratio (a/h) and aspect ratio (a/b) on the dimensionless frequency of a FG nanoplate with fully simply-supported and fully

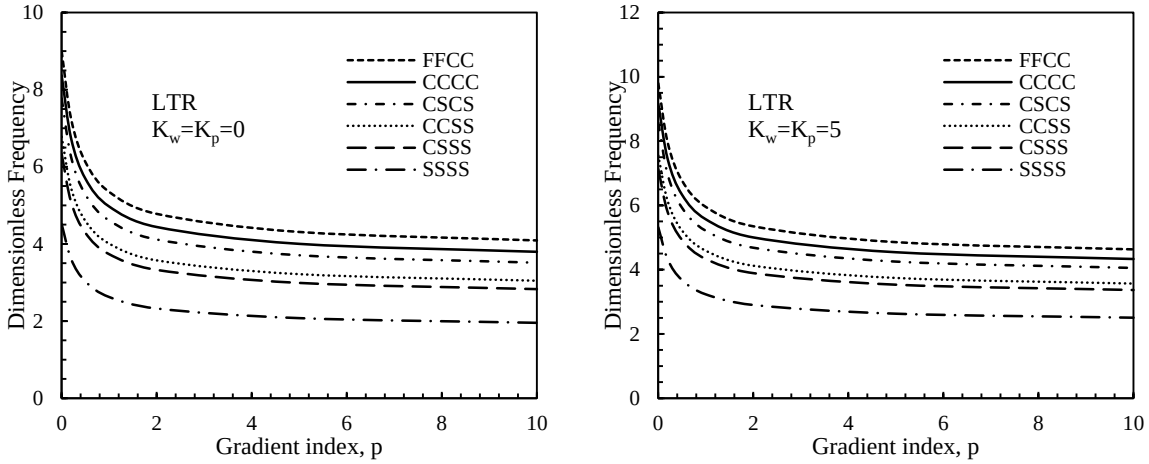

Fig. 7 Influence of material composition on the dimensionless frequency of square FG nanoplate for various thermal loadings and boundary conditions (μ=2, a/h=20, ΔT=100(K))

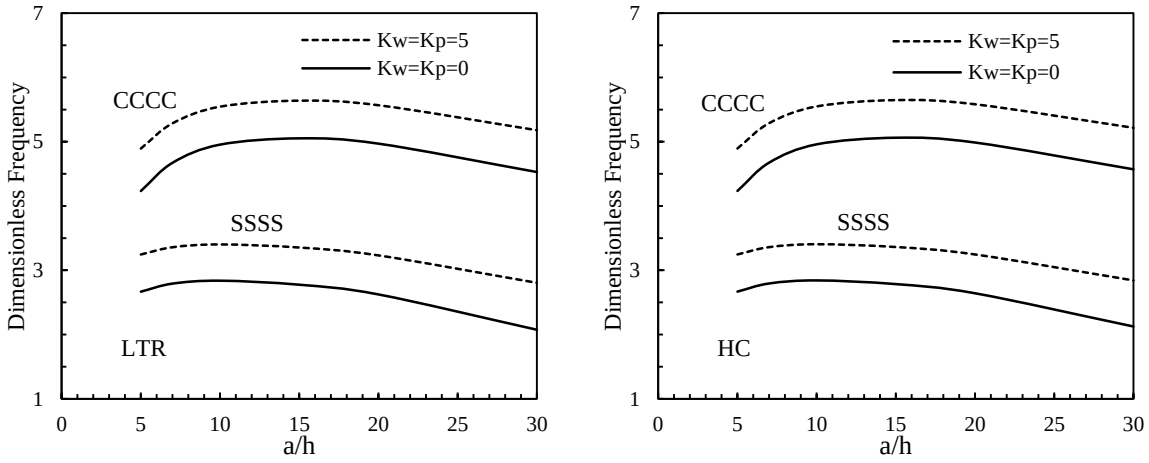

Fig. 8 Influence side-to-thickness ratio on the dimensionless frequency of square FG nanoplate for different thermal loadings (μ=2, p=1, ΔT=100(K))

clamped boundary conditions resting or not on elastic foundation at ΔT=100(K) and μ=2 nm^2. In both cases an increase in the Winkler or Pasternak parameters of elastic foundation supplies higher stiffness as well as natural frequency. Also, it is seen from the figures that for all types of thermal loading the dimensionless frequency arises for lower values of a/h and then diminishes with reducing plate thickness or increasing the value of a/h. While, with the increase of aspect ratio a/b the dimensionless frequency increases significantly.

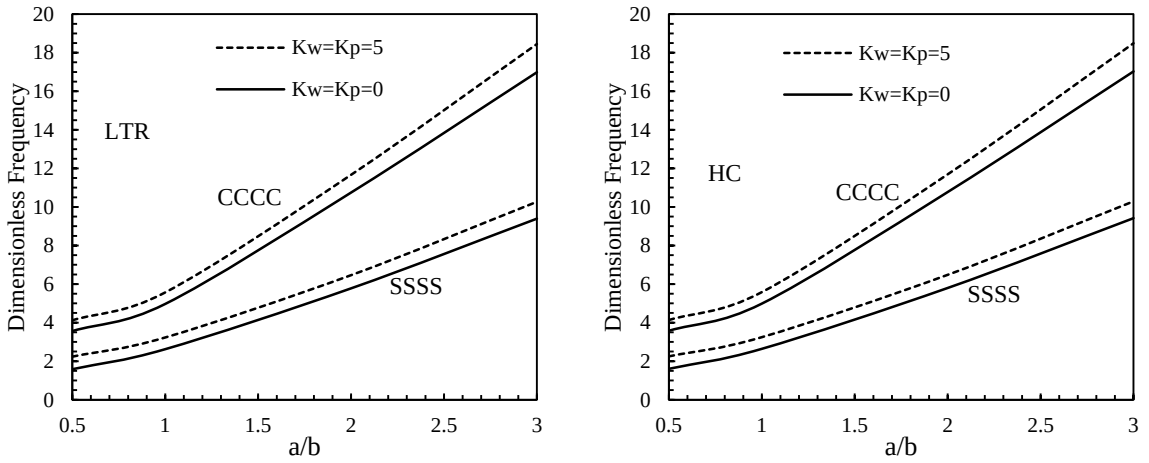

Fig. 9 Influence of aspect ratio on the dimensionless frequency of FG nanoplate for different thermal loadings (μ=2, p=1, ΔT=100(K))

6. Conclusions

The prime aim of the current work is to predict thermal vibration behavior of embedded temperature-dependent FG nanoplates based on four-variable plate theory. Two types of thermo-mechanical loading including linear and non-linear temperature rise are assumed. The material properties of a FG nanoplate are supposed to be temperature-dependent and they are graded according to Mori-Tanaka homogenization technique. By implementing extended Hamilton's principle, the nonlocal governing equations are derived based on a new trigonometric four-variable shear deformation plate theory. An analytical solution which satisfies various boundary conditions is then used to solve the equations. Several numerical examples are given to illustrate the impacts of elastic foundation, temperature-dependency, different thermal loadings, nonlocal parameter, gradient index, aspect and side-to-thickness ratio on the thermo-mechanical vibration behavior of FG nanoplates. It is indicated that, the dimensionless frequency of a FG nanoplate tends to zero near a prescribed temperature, which is known as critical temperature. It was found that a way to postpone the critical temperature is to increase the elastic foundation parameters. Also, various thermal loadings estimate different values of natural frequency and branching point so that linear temperature rise produce smaller natural frequency than non-linear temperature rise.

References

Ansari, R., Ashrafi, M.A., Pourashraf, T. and Sahmani, S. (2015), "Vibration and buckling characteristics of functionally graded nanoplates subjected to thermal loading based on surface elasticity theory", *Acta. Astronautica*, **109**, 42-51.

Barati, M.R., Zenkour, A.M. and Shahverdi, H. (2016), "Thermo-mechanical buckling analysis of embedded nanosize FG plates in thermal environments via an inverse cotangential theory", *Compos. Struct.*, **141**, 203-212.

Bouiadjra, R.B., Bedia, E.A. and Tounsi, A. (2013), "Nonlinear thermal buckling behavior of functionally graded plates using an efficient sinusoidal shear deformation theory", *Struct. Eng. Mech.*, **48**(4), 547-567.
Bourada, M., Tounsi, A. and Houari, M.S.A. (2012), "A new four-variable refined plate theory for thermal buckling analysis of functionally graded sandwich plates", *J. Sandw. Struct. Mater.*, **14**(1), 5-33.
Daneshmehr, A. and Rajabpoor, A. (2014), "Stability of size dependent functionally graded nanoplate based on nonlocal elasticity and higher order plate theories and different boundary conditions", *Int. J. Eng. Sci.*, **82**, 84-100.
Ebrahimi, F. and Barati, M.R. (2016), "A nonlocal higher-order shear deformation beam theory for vibration analysis of size-dependent functionally graded nanobeams", *Arab. J. Sci. Eng.*, **41**(5), 1679-1690.
Eltaher, M.A., Emam, S.A. and Mahmoud, F.F. (2012), "Free vibration analysis of functionally graded size-dependent nanobeams", *Appl. Math. Comput.*, **218**(14), 7406-7420.
Eringen, A.C. (1983), "On differential equations of nonlocal elasticity and solutions of screw dislocation and surface waves", *J. Appl. Phys.*, **54**(9), 4703-4710.
Eringen, A.C. and Edelen, D.G.B. (1972), "On nonlocal elasticity", *Int. J. Eng. Sci.*, **10**(3), 233-248.
Javaheri, R. and Eslami, M.R. (2002), "Thermal buckling of functionally graded plates based on higher order theory", *J. Thermal. Stress.*, **25**(7), 603-625.
Jung, W.Y., Han, S.C. and Park, W.T. (2014), "A modified couple stress theory for buckling analysis of S-FGM nanoplates embedded in Pasternak elastic medium", *Compos. Part B: Eng.*, **60**, 746-756.
Kim, S.E., Thai, H.T. and Lee, J. (2009), "A two variable refined plate theory for laminated composite plates", *Compos. Struct.*, **89**(2), 197-205.
Kulkarni, K., Singh, B.N. and Maiti, D.K. (2015), "Analytical solution for bending and buckling analysis of functionally graded plates using inverse trigonometric shear deformation theory", *Compos. Struct.*, **134**, 147-157.
Mechab, I., Atmane, H.A., Tounsi, A. and Belhadj, H.A. (2010), "A two variable refined plate theory for the bending analysis of functionally graded plates", *Acta Mechanica Sinica*, **26**(6), 941-949.
Nami, M.R. and Janghorban, M. (2014), "Resonance behavior of FG rectangular micro/nano plate based on nonlocal elasticity theory and strain gradient theory with one gradient constant", *Compos. Struct.*, **111**, 349-353.
Narendar, S. (2011), "Buckling analysis of micro-/nano-scale plates based on two-variable refined plate theory incorporating nonlocal scale effects", *Compos. Struct.*, **93**(12), 3093-3103.
Natarajan, S., Chakraborty, S., Thangavel, M., Bordas, S. and Rabczuk, T. (2012), "Size-dependent free flexural vibration behavior of functionally graded nanoplates", *Comput. Mater. Sci.*, **65**, 74-80.
Shen, H.S. and Wang, H. (2015), "Nonlinear bending and postbuckling of FGM cylindrical panels subjected to combined loadings and resting on elastic foundations in thermal environments", *Compos. Part B. Eng.*, **78**, 202-213.
Shimpi, R. P. (2002), "Refined plate theory and its variants", *AIAA J.*, **40**(1), 137-146.
Sobhy, M. (2013), "Buckling and free vibration of exponentially graded sandwich plates resting on elastic foundations under various boundary conditions", *Compos. Struct.*, **99**, 76-87.
Sobhy, M. (2014), "Generalized two-variable plate theory for multi-layered graphene sheets with arbitrary boundary conditions", *Acta. Mechanica*, **225**(9), 2521-2538.
Sobhy, M. (2015a), "Levy-type solution for bending of single-layered graphene sheets in thermal environment using the two-variable plate theory", *Int. J. Mech. Sci.*, **90**, 171-178.
Sobhy, M. (2015b), "Hygrothermal deformation of orthotropic nanoplates based on the state-space concept", *Compos. Part B. Eng.*, **79**, 224-235.
Sobhy, M. (2015c), "A comprehensive study on FGM nanoplates embedded in an elastic medium", *Compos. Struct.*, **134**, 966-980.
Sobhy, M. (2016), "An accurate shear deformation theory for vibration and buckling of FGM sandwich plates in hygrothermal environment", *Int. J. Mech. Sci.*, **110**, 62-77.
Ta, H.D. and Noh, H.C. (2015), "Analytical solution for the dynamic response of functionally graded rectangular plates resting on elastic foundation using a refined plate theory", *Appl. Math. Model.*, **39**(20), 6243-6257.

Thai, H.T. and Choi, D.H. (2011), "A refined plate theory for functionally graded plates resting on elastic foundation", *Compos. Sci.Tech.*, **71**(16), 1850-1858.

Thai, H.T. and Kim, S.E. (2012), "Levy-type solution for free vibration analysis of orthotropic plates based on two variable refined plate theory", *Appl. Math. Model.*, **36**(8), 3870-3882.

Touloukian Y.S. (1967), *Thermo-physical Properties Research Center. Thermo-physical properties of high temperature solid materials*, Vol. 1, Elements.-Pt. 1, Macmillan.

Tounsi, A., Houari, M.S.A. and Benyoucef, S. (2013), "A refined trigonometric shear deformation theory for thermoelastic bending of functionally graded sandwich plates", *Aero. Sci. technol.*, **24**(1), 209-220.

Zare, M., Nazemnezhad, R. and Hosseini-Hashemi, S. (2015), "Natural frequency analysis of functionally graded rectangular nanoplates with different boundary conditions via an analytical method", *Meccanica*, **50**(9), 2391-2408.

Zenkour, A.M. and Sobhy, M. (2011), "Thermal buckling of functionally graded plates resting on elastic foundations using the trigonometric theory", *J. Thermal. Stress.*, **34**(11), 1119-1138.

CC